JOURNAL OF THE BALKAN GEOPHYSICAL SOCIETY, Vol. 4, No 4, November 2001, p. 101-110, 9 figs.

Evaluation of Akdag iron ore reserves using Differential Markov Random Field (DMRF)*

Osman N. Ucan[1] and A. Muhittin Albora[2]

[1] University of Istanbul Department of Electrical Engineering Avcilar, 34850, Istanbul, Turkey E-mail: uosman@istanbul.edu.tr
[2] University of Istanbul Department of Geophysics Engineering Avcilar, 34850, Istanbul, Turkey E-mail: muhittin@istanbul.edu.tr

(Received 1 April 2000; accepted 5 January 2001)

Abstract: *In this paper, a contemporary image processing novel, Differential Markov Random Field (DMRF) has been applied to Bouguer anomaly map of Akdag iron ore reserves. DMRF is an appropriate unsupervised, stochastic and real time approach, which can specify the local properties of anomaly maps. DMRF obtains regional or residual anomaly maps using both neighbourhood relation and stochastic property of the Bouguer anomaly map. Dominant structures forming anomalies can be detected altering quantisation parameter of DMRF. The results of DMRF approach applied to Akdag iron ore reserves, have matched to Technical Ore Research of Turkey (MTA) reports.*

Keywords*: Differential Markov Random Field (DMRF), Akdag Bouguer Anomaly.*

INTRODUCTION

In our study area, two techtonostratigraphically diverse entities may be distinguished in Northern Anatolia (Fig. 1). These are (1) A Northern area termed the Pantide zone; and (2) A Southern area termed the Anatolides (Arni, 1939), the Taurides (Egeran, 1947; Ketin, 1966) or Anatolide platform (Sengor and Yilmaz, 1981). Elmas (1996) suggested that the Mesozoic paleogeography of the Eastern Pontides was defined by the Neotethys ocean between the two continental assemblages in the North and South. During the late Cenomanian/Turonian to Eocene, an island arc evolved as a result of N-dipping subduction of Neotethys. The ophidite-melange association was abducted onto the Pantide continent as a retrocharriage process in the Turanian-Maastrichtian, Paleocene, and the end of the early Eocene, and onto the Southern continent in Campanien-Maastrichtian and pre-late Lutetian time. We worked in Sivas-Divrigi region which is situated on the Southern tectonic unit and the ophialite-melange association.

The autochtonous basement of the region composed of quartz schist-phyllite (Hornovil Metamorphies) Triassic in age, and uncomformably overlying them a limestone sequence (Akdag limestone) Jurassic in age. Various types of ore mineralization were developed depending on the subalkaline-alkaline arc granitoids and related lamprophyre dikes, intruded the Divrigi ultrabasics seated on the basement in the Campanian. The listwaenitic rocks grown in tectonic zones of the ultrabasic rocks are poor in gold, cobalt and cupper (Onder and Yildizeli, 1985).

One of the main purposes of geophysical mapping is the identification of units that can be related to the unknown geology. On a regional scale, aeromagnetic and gravity maps are most useful tools presently available, although other techniques such as conductivity mapping (Palacky, 1986) or remote sensing (Watson, 1985) are very helpful in locating lithologic boundaries. Gravity anomaly separation can be effected by such wavelength filtering when gravity response from the geologic feature of interest (the signal) dominates one region (or spectral band) of the observed gravity field's power spectrum. Pawlowski and Hansen (1990) have investigated a gravity anomaly separation method based on frequency-domain Wiener filtering. Shu-Kun *et al.* (1996) has presented a method for geological boundaries from potential-field anomalies. Ucan *et al*. (2000) has applied wavelet approach to magnetic anomaly fields.

The objective of modelling in image analysis is to capture the instrinstic character of images in a few parameters so as to understand the nature of the phenomenon generating the images. Image models are also useful in quantitatively specifying natural constraints and general assumptions about physical world and the imaging

* This work was supported by Research Institute of Istanbul University. The project number:1247/050599

process. The introduction of stochastic models in image analysis has led to many practical algorithms that would have been revised with ad-hoc processing. Over the last few years a growing number of researches in image analysis, applied mathematics and statistics have used Markov random field models.

In this paper, we have introduced a new unsupervised image processing novel named as Differential Markov Random Field (DMRF). DMRF obtains regional or residual anomaly maps using both neighbourhood relation and stochastic property of the Bouguer anomaly map. It does not require a priory knowledge on the image and the number of regions or classes need not to be known. Dominant structures forming anomalies can be detected altering quantisation parameter of DMRF. Thus residual or regional separation performance of DMRF approach can be increased with choosing the best-fit quantisation level. We applied our new approach to a real data, Akdag iron ore region, and DMRF outputs matched to Technical Ore Research of Turkey (MTA) reports.

DIFFERENTIAL MARKOV RANDOM FIELD (DMRF) APPROACH

The Bouguer anomaly of geological regions, generally has low signal to noise ratio and there is background clutter and noise related with the different characterised geological structures. The classical approaches use local pixel intensity information to identify whether a pixel location is part of a boundary. Filters are used to collect local gradient information and, if the magnitude of the local gradient is large enough, the pixel is declared an edge pixel. Unfortunately, such techniques are sensitive to noise and, in addition, global boundary information is not available, which hinders the determination of closed objects boundaries.

The stochastic models depending on Markov Random Field (MRF) approach in 2-D data analysis has led to the development of many practical algorithms (Dubes *et al*., 1989, Geman and Geman, 1984; Derin and Elliot, 1987) that would not have been realised with *ad-hoc* processing. A random field is a joint distribution imposed on a set of random variables representing objects of interest, such as pixel intensities, that imposes the statistical dependence in a spatially meaningful way.

The objective of modelling is to capture the intrinsic character of data in a few parameters so as to understand the nature of phenomenon generating the data. The literature of 2-D data analysis has been experienced a resurgence in the use of stochastic models to represent image data and to express prior, generic knowledge. Given a realisation of a Gibbs Random Field (GRF) and a

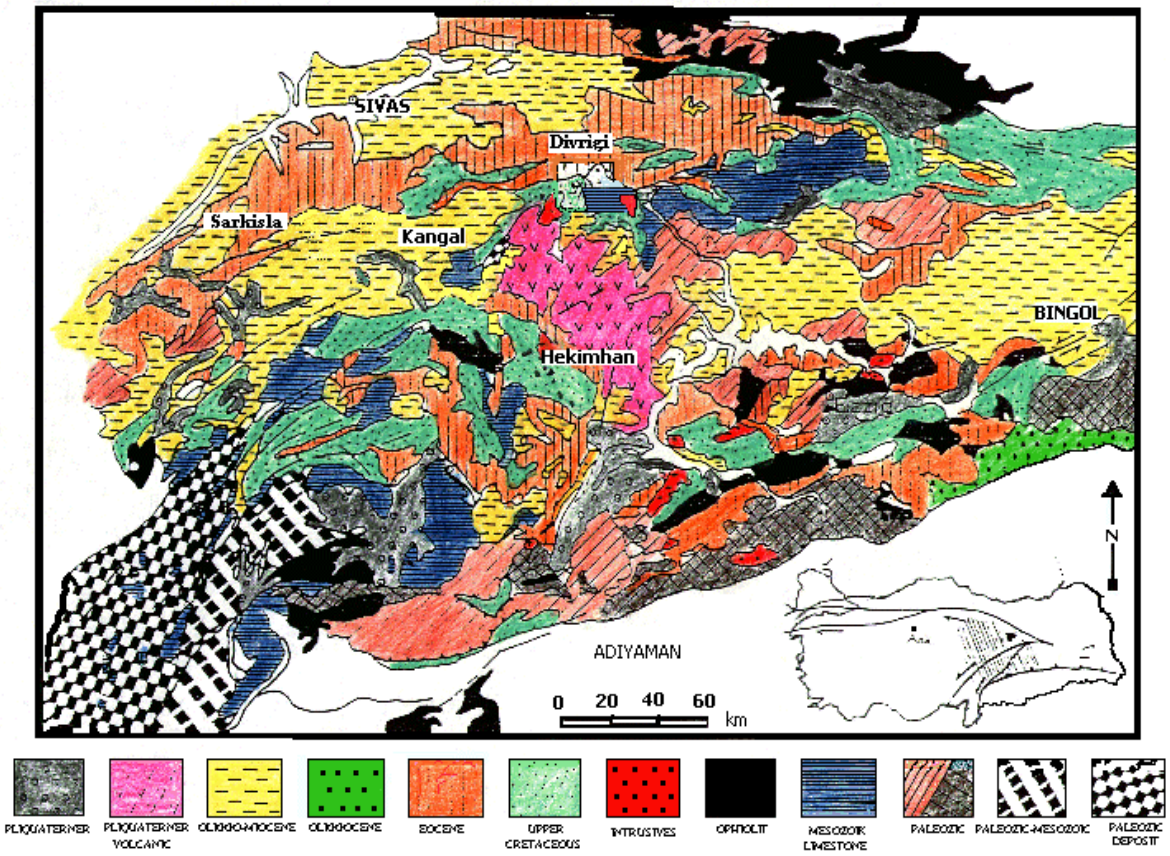

FIG. 1. General geological map of Akdag region (Ozturk, 1991).

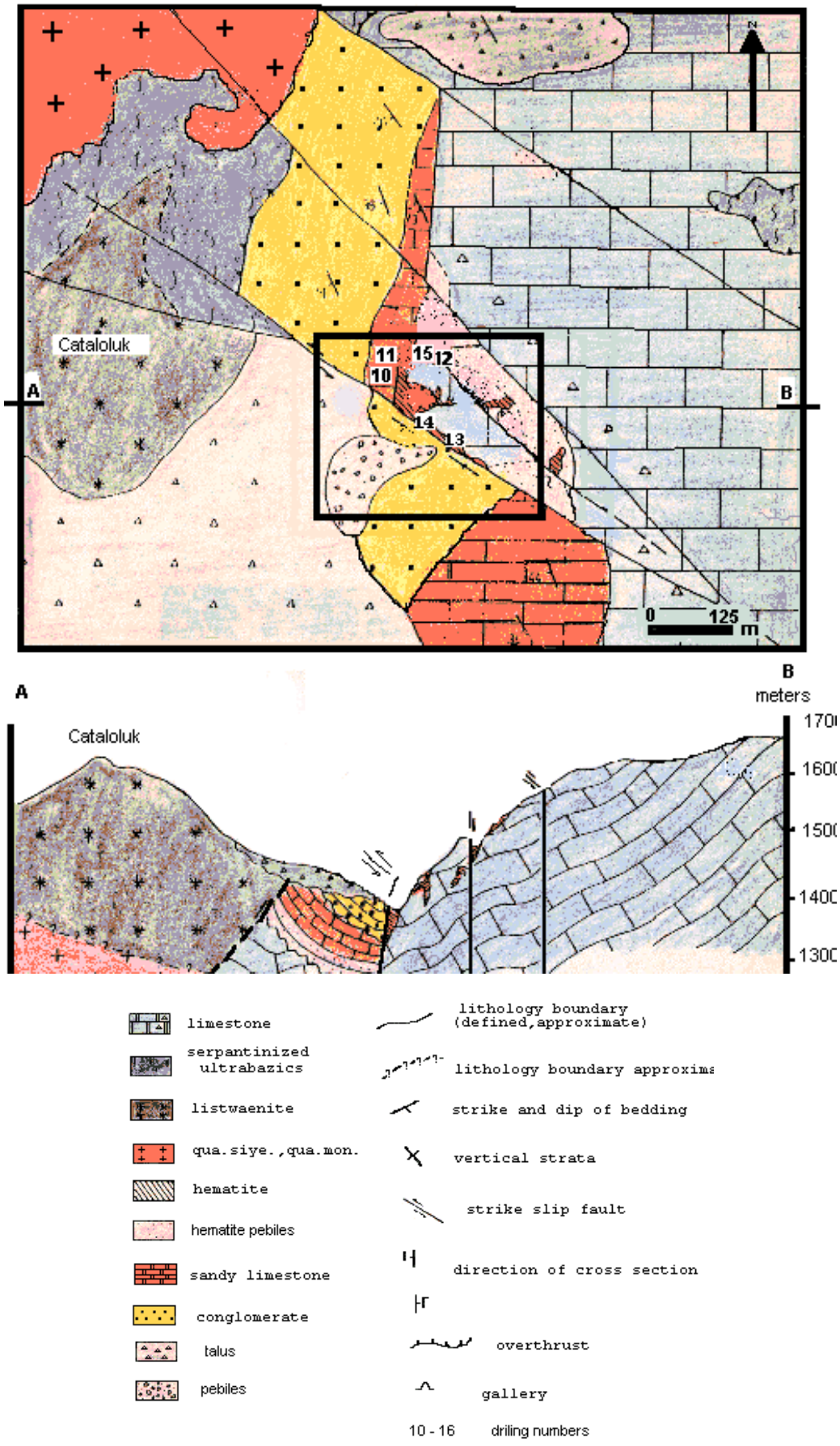

FIG. 2. Geological map of Akdag iron ore and its horizontal cross-section (Ozturk, 1991).

defined model, we examine procedures for estimating the parameters in this GRF. Since only one realisation is available and a complicated partition function is involved, the traditional statistical estimation methods are infeasible.

In recent years, there has been increasing interest in use of statistical techniques for modelling and processing data. The reports by Dubes *et al*., (1989), Geman and Geman, (1984), Derin and Elliot, (1987), all make use of the Gibbs distribution (GD) for characterizing MRF. This paper presents a new approach to the application of GD for problems in gravity anomaly maps. So we give the basic definitions of GD and a particular class of GD used in gravity separation.

Basic definitions of Gibbs distributions

Gravity anomaly map, we investigate is assumed to be a finite $N_1 X N_2$ rectangular *lattice* of points (pixels) defined as $L = \{(i, j) : 1 \le i \le N_1, 1 \le j \le N_2\}$. A collection of subsets of L described as,

$$\eta = \{\eta_{ij} : (i, j) \in L, \eta_{ij} \subseteq L\} \quad (1)$$

is a neighbourhood system on L if and only if η_{ij} the neighbourhood of pixel (i,j) is such that

- $(i, j) \notin \eta_{ij}$
- if $(k,l) \in \eta_{ij}$ then $(i, j) \in \eta_{kl}$ for any $(i, j) \in L$.

A hierarchically ordered sequences of neighbourhood systems that are commonly used in modelling are $\eta^1, \eta^2, ..., \eta^l = \{\eta_{ij}^l\}$ consisting of the closest four neighbours of each pixel known as nearest-neighbour model (Derin and Elliot, 1987). $\eta^2 = \{\eta_{ij}^2\}$ is such that $\{\eta_{ij}^2\}$ consists of eight pixels neighbouring (i,j). The usual neighbourhood system in image analysis defines the first-order neighbours are the four pixels sharing a side within the given pixel. Second-order neighbours are the four pixels sharing a corner. Higher order neighbours are defined in an analogues manner. The neighbourhood structures are given in Figure 3 and 4. The neighbourhood system η^m is called the m^{th} order neighbourhood system.

A clique is a set of sites in which all pairs of sites are mutual neighbourhood relations are defined in the probabilistic sense. The cliques related with a lattice-neighbourhood pair (L,η), denoted by c, is a subset of L such that

- c consists of a single pixel, or
- for $(i, j) \ne (k,l), (i, j) \in c$ and $(k,l) \in c$ implies that $(i, j) \in \eta_{kl}$.

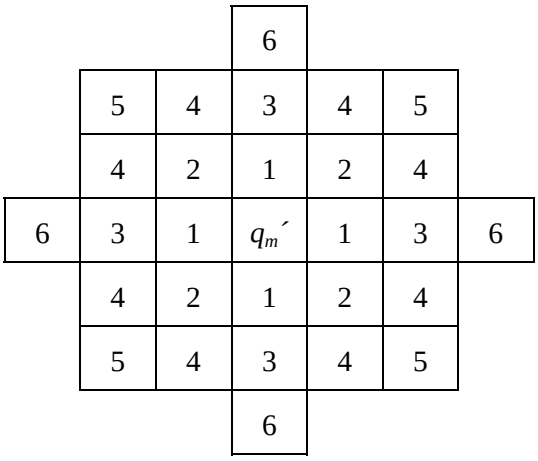

FIG. 3. Hierarchially arranged neighbourhood system η^m

The collection of all cliques of (L,η) is denoted by C = C(L,η). The types of cliques associated with η^1 and η^2 are shown in Figure 4.

Let η be a neighbourhood system defined over the finite lattice L. A random field $X = \{X_{ij}\}$ defined on L has *Gibbs Distribution* (GD) or equivalently is a *Gibbs Random Field* (GRF) with to η if and only if its joint distribution is of form,

$$P(X = x) = \frac{1}{Z} e^{-U(x)}, \quad (2)$$

where

$U(x) = \sum_{c \in C} V_c(x)$, defined as *energy function*

$V_c(x)$ - potential associated with clique *c*.

Defining the global energy functions is a powerful tool for specifying nonlinear interactions between different image features. They help to combine and organise spatial and temporal information by introducing strong generic knowledge about the features to be estimated.

$Z = \sum_s e^{-U(x)}$ - partition function is simply a normalizing constant.

The joint distribution expression in (2) has the physical interpretation that the smaller energy function $U(x)$, the energy of the realization x, is the more likely that realization is [i.e., larger $P(X=x)$]. Minimizing the global energy function U is however usually a hard optimization problem: the number of possible label configurations is generally very large and moreover, the global energy function U may contain local minima. Computationally demanding stochastic relaxation algorithms are therefore generally necessary to compute exact maximum aposteriori probability (MAP) solutions.

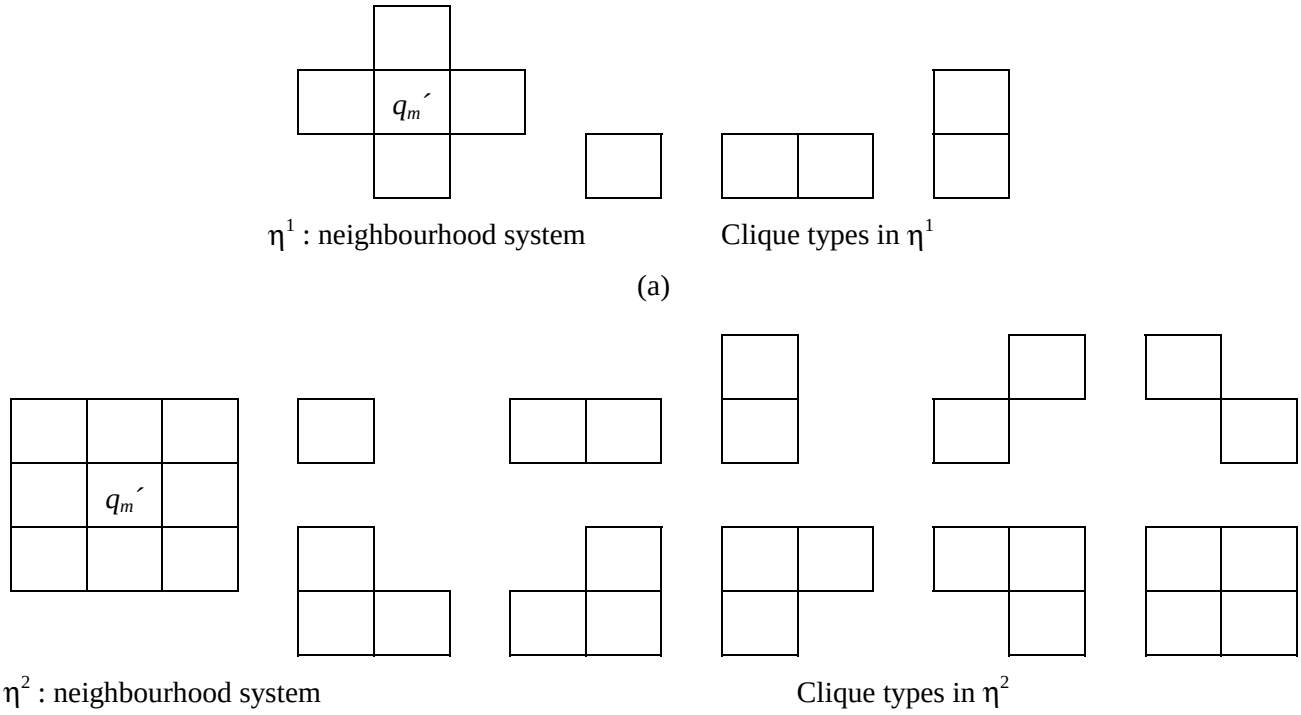

FIG. 4. Neighbourhood systems η^1 and η^2 and their associated clique types.

The GD is basically an exponential distribution. By choosing the clique potential $V_c(x)$ properly, a wide variety of distributions both for discrete and continous random fields can be formulated as GD. Besag, (1974) proved that there is one-to-one correspondence between Markov Random Field (MRF) and Gibbs Random Field (GRF). Then any random field can be considered as MRF, consequently as a GRF, with respect to a large enough neighbourhood system.

V_1	U_2	V_2
U_1	$\mathbf{q_m'}$	U_3
V_1	U_4	V_3

FIG. 5. q'_m and η_{ij} of Akdag Bouguer map.

Differential Markov Random Field model (DMRF) for gravity anomaly map

Differential Markov Random Field, DMRF is a very natural model that is able to translate local information and assumptions into a global model. In this paper, we describe a gravity anomaly map $y = \{y_{ij}\}$ as an N_1 X N_2 matrix of observations. It is assumed that this matrix y is a realization from a random field $Y = \{Y_{ij}\}$ which is the sum of gravity fields produced by all underground sources. In our case, the targets for specific surveys are often small-scale structures buried at shallow depths, and the scene including these targets are defined as a residual random field X = {Xij}. Contextual information enters through DMRF model is its statistical dependence among the neighbouring pixels. The random field X is a discrete valued random field, where X_{ij} takes values M quantisation level as defined $Q = \{q_1, q_2, q_3, ...q_M\}$. Dominant structures forming anomalies can be detected altering quantisation level parameter M of $Q = \{q_1, q_2, q_3, ...q_M\}$ and by choosing suitable quantisation level, residual or regional separation performance of DMRF approach can be improved.

Correct estimation and removal of the regional field from initial field observations yields the residual field produced by the target sources. Interpretation and numerical modelling are carried out on the residual field data, and the reliability of the interpretation depends to a great extent upon the success of the regional-residual separation. In other words, given a gravity anomaly map realization y, it is desired to determine residual scene x that given rise to y. The scene realization of x, of course, is not observed and can not be obtained deterministically from y. So the problem is to obtain an estimate $x^* = X^*(y)$ of the scene X, based on a realization y. Having set up the problem statistically, maximum a posteriori (MAP) estimation is chosen as statistical criterion (Derin and

Elliot, 1987). So the objective now is to have an estimation rule, that is, an algorithm, which will yield x^* that maximizes the a posteriori distribution $P(X = x|Y = y)$ for a given y. Applying Bayes' rule, the *a posteriori* distribution can be written as,

$$P(X = x|Y = y) = \frac{P(Y = y|X = x)P(X = x)}{P(Y = y)} \quad (3)$$

The model relating observation y to labelling x is chosen to ensure that the posterior distribution of X, given $Y = y$ is also a MRF. The sampling algorithms can be exploited in the estimation process. Since probability, $P(Y=y)$ does not effect maximization, logaritmic of Equation (3) can be written as,

$$\ln P(X = x, Y = y) = \ln P(X=x) + \ln P(Y = y|X = x) \quad (4)$$

To maximize Equation (4) for gravity anomaly maps, we proposed Differential Markov Random Field (DMRF) approach since in gravity anomalies at the boundaries of regions of the original data, residual information is carried. Gravity anomaly map, we investigate is assumed to be a finite $N_1 X N_2$ rectangular lattice of points (pixels) defined as {yij} are passed through a Differential Markov Random Field (DMRF) precoder resulting $\{s_{ij}\}$ parameters as,

$$s_{ij} = \left| M y_{ij} - \sum_i \sum_j \eta_{ij} \right|, \quad (5)$$

where M is the number quantisation levels obtained at residual map. η_{ij} the neighbourhood of pixel (i,j). Then the two components of the joint log-likelihood in (4) can be expressed for DMRF as,

$$\ln \mathrm{P(Y = y|X =x)} = \\ = -\frac{N_1 N_2}{2} \ln(2\pi\sigma^2) - \sum_{m=1}^{M} \sum_{(i,j)\in S_m} \frac{1}{2\sigma^2} (s_{ij} - q_m')^2 \quad (7)$$

where $S_m=\{(i,j) \in L : X_{ij} = m\}$. Z is defined at Equation (2), $q_m' \in q_m$ is the transient quantisation level of residual map during optimisation, and $V_c(x)$ is the potential associated with clique c. The joint log-likelihood $\ln P(X=x,Y=y)$ (Equation 4) is the sum of (6) and (7) and is to be optimized. Then we need to compute the second component of Equation (6). Using similar optimisation approach of Derin and Elliot (1987), we present the formulation in terms of a second order neighbourhood system η^2, although its extension to any order is possible. Consider a site (i,j) and its neighbourhood η_{ij} at residual map of X. Let q_m' is the transient quantisation level of residual map during optimisation at (i,j) pixel and t' represent the vector of neighboring values of q_m' at (i,j).

$$t' = [u_1, u_2, u_3, u_4, v_1, v_2, v_3, v_4]^T, \quad (8)$$

where the location of u_i's and v_i's with respect to q_m' are shown in Figure 3. We define indicator functions,

$$\mathrm{I}(z_1, z_2, ..., z_k) = \begin{cases} -1 & , \quad z_1 \approx z_2 \\ 1 & , \quad \text{otherwise} \end{cases} \quad (9)$$

$\approx$ is the approximation defined as,

$$z_k \approx z_{k+1} \equiv |z_k - z_{k+1}| \le \varepsilon, \quad (10)$$

where ε is a small value given regarding to optimisation tolerance. Another indicator $J_m(q_m')$ is defined as,

$$\mathrm{J_m}(q_m') = \begin{cases} -1. & , \quad q_m' \approx q_m \\ 1 & , \quad \text{otherwise} \end{cases} \quad (11)$$

Using these indicators we can express the potential function (6) of all cliques that contain (i,j), the site of q_m' (Fig. 5). That is

$$V(q_m', t', \theta) \equiv \sum_{c:q_m' \in C} V_C(x) \quad (12)$$

where θ is the parameter vector. Thus both (6) and (7) are defined as a function of q_m', resulting common optimisation which improves the DMRF performance greatly.

θ is defined as,

$$\theta = [\alpha_1, \alpha_2, .., \alpha_M, \beta_1, \beta_2, \beta_3, \beta_4, \gamma_1, \gamma_2, \gamma_3, \gamma_4, \xi_1]^T \quad (13)$$

Then we can rewrite (12) as,

$$V(q_m', t', \theta) \equiv \phi^T(q_m', t')\theta, \quad (14)$$

where

$$\begin{aligned} \phi(q_m', t') = [&J_1(q_m'), J_2(q_m'), \ldots J_M(q_m'), (I(q_m', u_1) + \\ &+ I(q_m', u_3)), (I(q_m', u_2) + I(q_m', u_4)), (I(q_m', v_2) + \\ &+ (I(q_m', v_4)), (I(q_m', v_1) + I(q_m', v_3)), (I(q_m', u_2, v_2) + \\ &+ I(q_m', u_4, u_3) + I(q_m', u_1, v_4)), (I(q_m', u_4, v_3) + \\ &+ I(q_m', u_2, u_3) + I(q_m', u_1, v_1)), (I(q_m', u_2, v_1) + \\ &+ I(q_m', u_1, u_4) + I(q_m', u_3, v_3)), (I(q_m', u_1, u_2) + \\ &+ I(q_m', u_4, v_4) + I(q_m', u_3, v_2)), (I(q_m', u_1, v_1, u_2) + \\ &+ I(q_m', u_2, v_2, u_3) + I(q_m', u_3, v_3, u_4) + I(q_m', u_4, v_4, u_1))]^T \end{aligned} \quad (15)$$

Suppose $P(q_m', t')$ is the joint distribution of random variables on 3x3 block centered at (i,j) and $P(t')$ is the joint distributions on η_{ij} only. Then the conditional probability, using Bayes' rule can be written as,

$$\frac{P(q_m', t')}{P(t')} = P(q_m'|t') = \frac{e^{-V(q_m', t', \theta)}}{W(t', \theta)}, \quad (16)$$

where

$$W(t', \theta) \equiv \sum_{s \in Q} e^{-V(q_m', t', \theta)}. \quad (17)$$

Rearranging (16)

$$\frac{e^{-V(q_m', t, \theta)}}{P(q_m', t')} = \frac{W(t', \theta)}{P(t')} \quad (18)$$

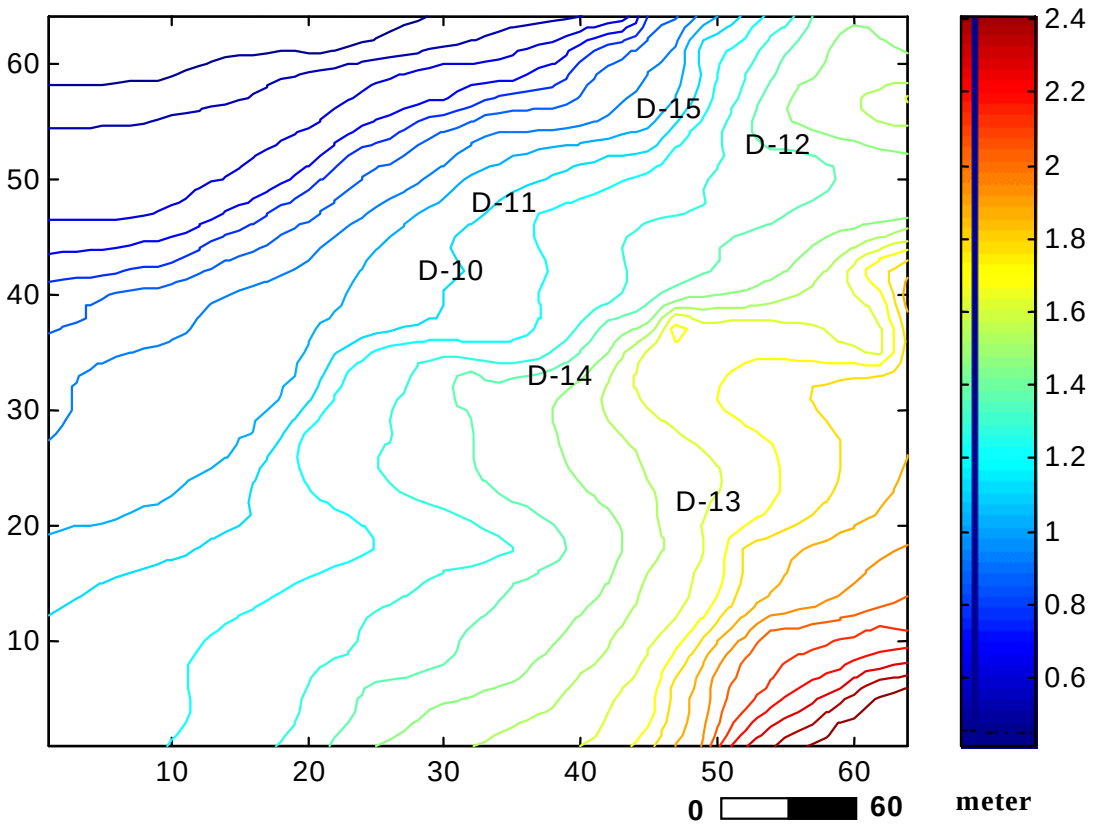

FIG. 6. Bouguer Anomaly of Akdag iron ore reserves (Dogan *et al*., 1989).

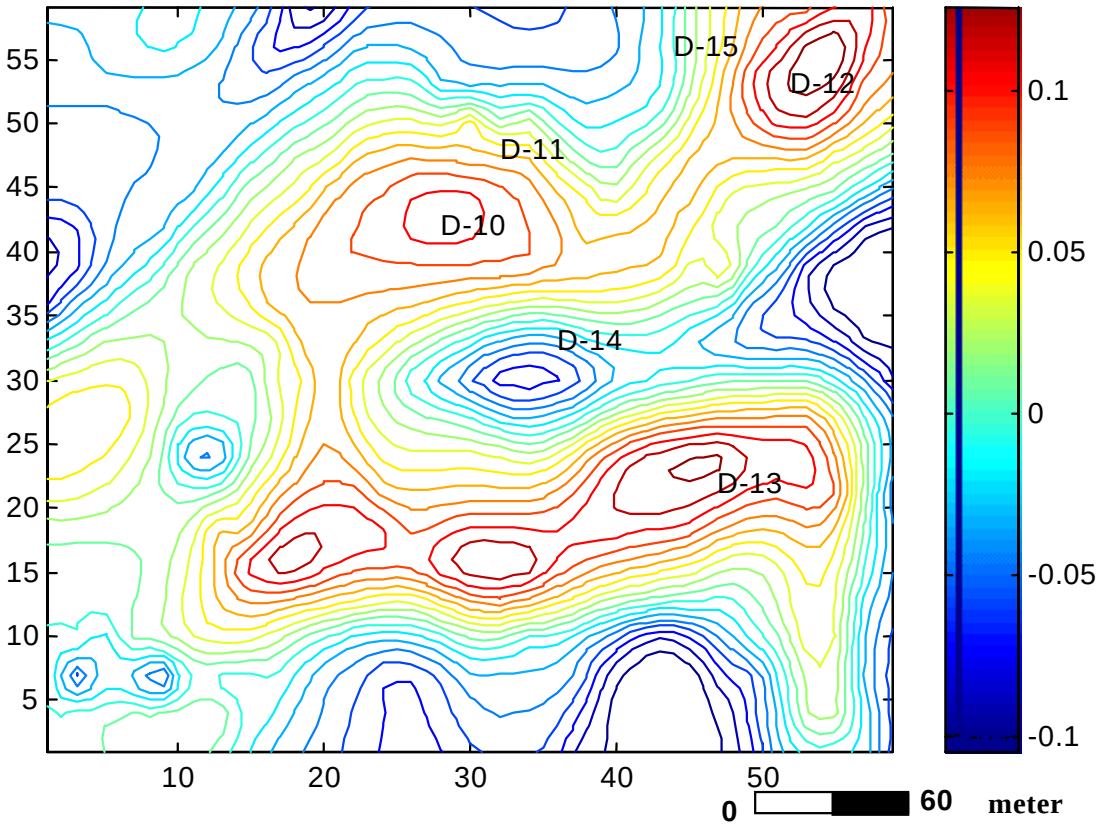

FIG. 7. Classical derivative method Applied to Akdag Iron Ore (Dogan *et al*., 1989).

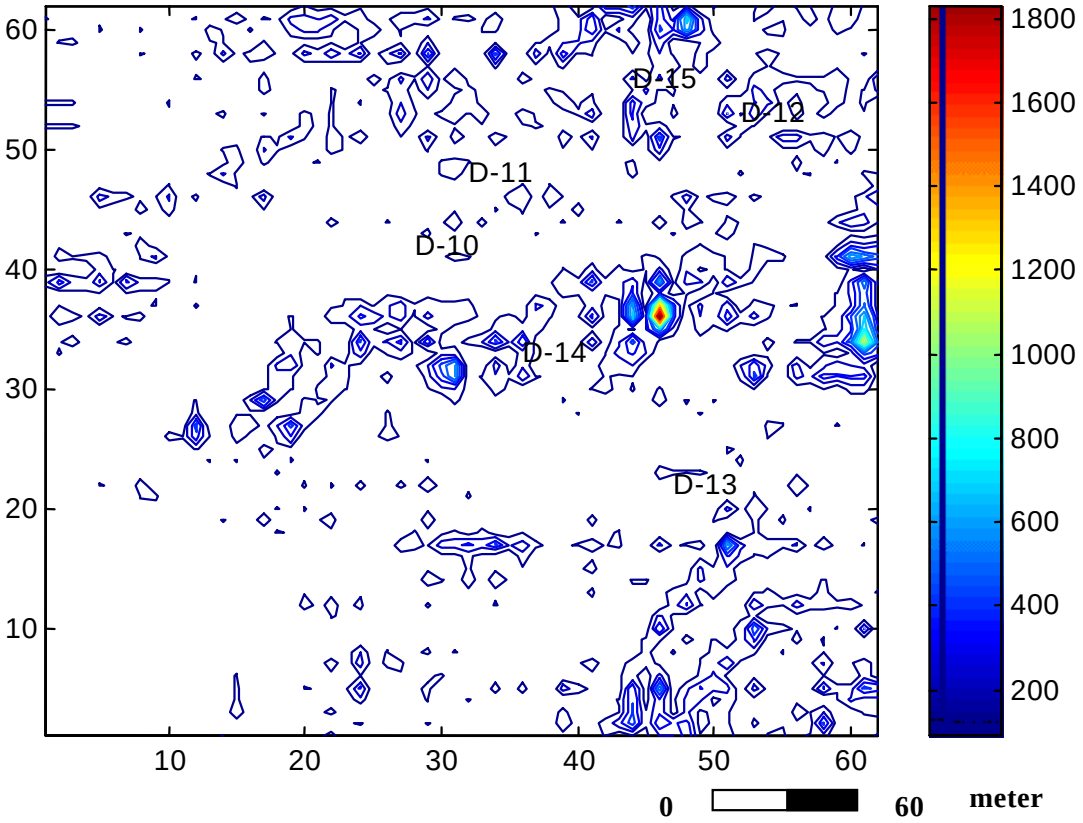

FIG. 8. DMRF output of the Bouguer Anomaly given in Figure 6 for quantisation level 8.

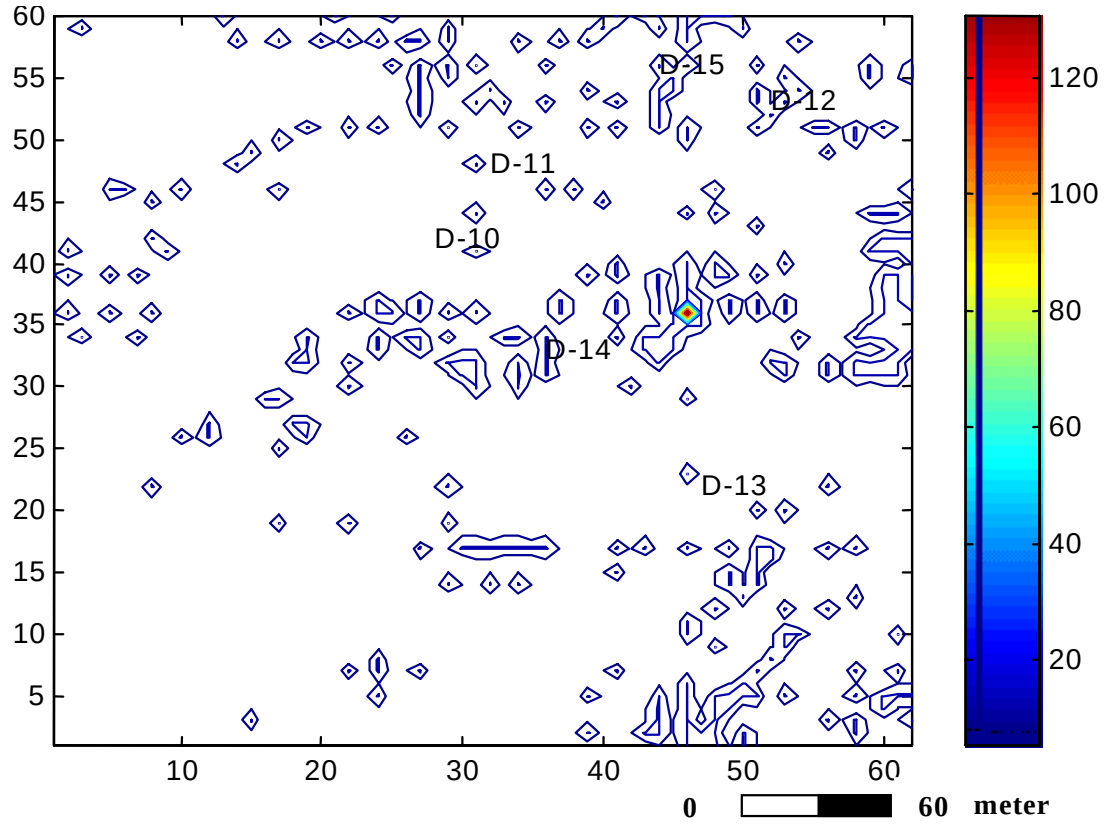

FIG. 9. DMRF output of the Bouguer Anomaly given in Figure 6 for quantisation level 6.

is obtained. Considering only left hand side of Equation (18), for two distinct values of $q'_m = j$, $q'_m = k$ values we have,

$$e^{-V(j,t',\theta)+V(k,t',\theta)} = \frac{P(j,t')}{P(k,t')} \quad (19)$$

Taking the natural logarithm of (19) and replacing (14), we obtain,

$$(\phi(k,t') - \phi(j,t'))^T \theta = \ln(\frac{P(j,t')}{P(k,t')}) \quad (20)$$

In (20), the vector $(\phi(k,t') - \phi(j,t'))$ is determined easily for any j, k, t' while θ is the unknown parameter to be estimated. The question that remains to be replied is how to determine $P(q'_m,t')$ values. We achieve this using histogram techniques. As a result, we have explained how to extract residual gravity map using Differential Markov Random Field approach.

AKDAG IRON ORE ANOMALY SEPARATION USING DIFRENSION MARKOV RANDOM FIELD

In this section, we have applied DMRF approach to the Bouguer anomaly of Akdag iron ore data as in Figure 6. Sivas-Divrigi Region, Akdag iron ore is composed of oxide and covering carbonated iron minerals. Sulphur mineral has not been observed. Albora, (1992) has modelled geophysical structure of Sivas region using nomogram method. A mass production of approximately 1.5 million ton qualified hematite has been achieved till 1992. The first drilling had been started by Technical Ore Research of Turkey (MTA) at 1962. After long studies, 880 000 ton definite ore and 294 000 ton possible ore deposists, totally 1 182 000 ton 60% tenorous iron ore has been estimated in this region. During 1963-1970 period, iron mineral production has been easily continued. In 1976 MTA, restarted its drilling projects and 428 000 ton definite ore and 150 000 ton possible ore deposists, totally 578 000 ton reserves have been estimated at Yildizeli Region of Sivas-Divrigi Area. In 1986, 250 000 ton iron ore deposist have been found after a new drillig log results. MTA is still continuing similar researches in the considered region.

Akdag iron ore basement is in the region of breccias with Mesozoic limestone. The breccias with limestones lies separately till the end of Kurugol area which places on the west bank of Akdag. Breccias limestones pieces has iron cement properties. As it is closer the original ore, the structure of the cutting becomes yellow like colour because of the lemonite and siderit concentration. Iron ore takes place in the 2-3 cm thickness of the zone having yellowish like brown as a result of the ore metazomatism. In the scientific researches it is found that the structure turns to be siderite lemonide and hematite by long period of time durations.

MTA has investigated these areas keenly and tried to separate residual anomaly by using classical derivation algorithms. MTA has drilled many logs, namely D10 to D-15 regarding the classical approach outputs (Fig. 7). Unfortunately, iron ore has been found only at D-15 drilling log (Dogan *et al.*, 1989). The other drillings are not productive although there observed anomalies in clasical derivative based modelling as shown in Figure 7.

Our new approach, DMRF takes into account not only neighbourhood ralations of pixels also stochastic propery of the input data requiring no training and no priory information about the image as expressed in Equations 6-7. The neighbourhood relation of the pixels helps us to combine pixels with similar anomaly values together to form image blobs and to decrease the input high level (mostly 256 level) image to a low quatised level, M. The stochastic property of the input image is used to derive out probability of similar blobs of the input data (Equation 20) and optimise Equations 6 and 7.

Here we have applied DMRF to Bouguer anomaly of iron ore at Akdag region. We evaluate Bouguer anomaly map as an input data with no prior information and no training about the considered image. It is clear that MRF type modellings do not require a priory knowledge of the input image (Derin and Elliot, 1987). There is also no training process since DMRF is real time and an unsupervised learning technique. We have evaluated the real data for different quantisation levels which can be thought as an DMRF parameter. Our aim is to find out the dominant effective ore coordinates and offer efficient drilling logs.

At the output of DMRF with quantisation level number 8, at the coordinates of D-10, D-11, D-13, and D-14, there seems to closed regions and no productive anomaly (Fig. 8). But at the D-15 coordinates, there is strongly separated residual anomaly showing iron ore. At the coordinated of D-12 a closed area is also obtained. The drilling shows also hematite ore with low density at D-12 drilling. Thus we can say that DMRF results match the physical drillings of MTA.

By decreasing quantisation level to 6, D-15 anomaly magnitude is now observed more easily (Fig. 9). So altering quantisation level as parameter, we can increase halftoning capability of the DMRF approach and dominant structures forming anomalies can be detected. As a result, we can conclude that our contemporary image processing algorithm matches with physical data of MTA Report.

ACKNOWLEDGEMENT

We thank the reviewers' comments, which helped us to improve our manuscript. This work was supported by Research Institute of Istanbul University, the project number 1409/050500.

CONCLUSION

In this paper, Differential Markov Random Field **(**DMRF) is introduced and applied to Bouguer anomaly map of Akdag iron ore reserves. In DMRF we pre-process the original data as a function of quantisation level M and neighbourhood ralationship. In our proposed scheme no training and priory information is necessary. It is an unsupervised, real time model. DMRF obtains regional or residual anomaly maps using both neighbourhood relationship and stochastic property of the Bouguer anomaly map. We can evaluate different properties of the image by altering quantisation parameter of DMRF.

As a real example, we have investigated Akdag iron ore which is about 12 km north of Sivas-Divrigi region and 700 m far east of of Cataloluk hill at the code of 1350-1600 m. The characteristics of Akdag ore has great differences compared to the other close regions in the view of its rockiness and ore quality. In this region, 1.7 million ton hematite is produced and the most qualified iron reserve area of Turkey. In this study, we work on the 1:1000 scaled Bouguer anomaly map as an input image (Fig. 6).

In 1977, MTA applied classical derivative methods for this region and residual anomaly map is obtained as shown in Figure 7. MTA has drilled many logs for the closed areas in Figure 7. The productive logs are only D-15 and partially D-12. In D-12, the well is 77 m depth and hematite ore is found in the zone of 58 m to 62 m. In D-15, the depth of the well is 76 m and hematite ore is in the range of 11-22 m depth.

We have evaluated the considered region using DMRF for quantisation level 6 and 8. At the output of DMRF with quantisation level number (M) 8, at the D-15 coordinates, there is strongly separated residual anomaly showing iron ore. At the coordinates of D-12 a closed area is also obtained (Fig. 8). For the quantisation level (M) 6, D-15 anomaly magnitude is now observed more easily (Fig. 9). In both quantisation level values, at the coordinates (45,36) of Figures 8 and 9, we have found the highest anomaly and we offer new drillings for the considered closed regions. As a result, we can conclude that our contemporary image processing algorithm outputs match with physical drilling data of MTA Reports.

REFERENCES

Albora, A. M., 1992. Evaluation of gravity anomaly of different geometric structures: Istanbul University, Science Institute, Master Thesis.

Arni, P., 1939. Tektonische Grundzuge Ostanatoliens und benachbarter Geiete: Meteae, series B, No.4, MTA-Ankara.

Besag, J., 1974. Spatial interaction and the statistical analysis of lattice systems, J.Roy: Statistics Soc. B, **36**, 192-236.

Derin, H. and Elliot, A. H., 1987. Modelling ans segmentation of noisy and textured images using Gibbs Random Field: IEEE PAMI, **9**, 39-55.

Dogan, H., Yildizeli N., Yurt, M.Z., Celebi, A. and Ozcen, H., 1989. T.D.C.I. Geological iron ore report 89/120 on Sivas Divrigi and its environment with project number AR: 33613-Poligon-II. IR:922 and with the support of TDCI General Management M.T.A., 89/120, Ankara.

Dubes, R. C. and Jain, A., 1989. Random field models in image analysis: Journal of applied Statistics, **16**, 131-162.

Egeran, N., 1947. Tektonique de la les Unite's Tectoniques et les Gites Metalliferes de la Turquie. Nancy, G.Thomas.

Elmas, A., 1996. Geological Evolution of Northern Anatolia: International Geology Review, **38**, 884-900.

Geman, S. and Geman, D., 1984. Stochastic Relaxation, Gibbs Distributions, and the Bayesian restoration of images: IEEE PAMI, **6**, 721-741.

Ketin, I., 1966. Cambriyen processing of south Anatolia and comparison of considued region with Iranien cambrien: MTA Journal, Number 66.

Onder, E. and Yildizeli, N., 1985. Geological report of Sivas-Divrigi Akdag iron ore horizon: M.T.A, Ankara.

Ozturk, H., 1991. Divrigi ore provence and source comments: Ph. D. Thesis, Istanbul University, Science and Technology Institutue.

Palacky, G. J., 1986. Geological background to resistivity mapping: Ed., Palacky, G. J., Airborne resistivity mapping: G.S.C., **86**-22, 19-27.

Pawlowski, R. S. and Hansen, R. O., 1990. Gravity anomaly separation by Wiener filtering: Geophysics, **55**, 539-548.

Sengor, A.M.C. and Yilmaz, Y., 1981. Tetyan evolution of Turkey, A plate tectonic approach: Tectonophysics, **75**,181-241.

Shu-Kun, H., Jean-Claude, S. and Chuen-Tien, S., 1996. High-resolution detection of geological boundaries from potential-field anomalies: An enhanced analytical signal technique: Geophysics, **61**, 373-386.

Ucan, O. N., Serhat, S., Albora, A. M. and Ozmen, A., 2000. Separation of Magnetic Field in Geophysical Studies Using 2-D Multi Resolution Wavelet Analysis Approach: Journal of the Balkan Geophysical Society, **3**, 3, 53-58.

Watson, K., 1985. Remote sensing: A geophysical perspective: Geophysics, **55**, 843- 50.